

LWP -985

~~FOR REFERENCE~~

LWP - 985
Copy No. 20

~~FOR NASA ONLY~~
~~FOR REFERENCE~~

LANGLEY WORKING PAPER

THE EFFECT OF SUSPENSION-LINE LENGTH
ON VIKING PARACHUTE INFLATION LOADS

By

Theodore A. Talay,

Lamont R. Poole,

and

Charles H. Whitlock

Langley Research Center
Hampton, Virginia

~~LIBRARY COPY~~

~~AUG 12 1971~~

LANGLEY RESEARCH CENTER
LIBRARY, NASA
HAMPTON, VIRGINIA

~~This paper is given limited distribution
and is subject to possible incorporation
in a formal NASA report.~~

NATIONAL AERONAUTICS AND SPACE ADMINISTRATION

September 2, 1971

September 2, 1971

LANGLEY WORKING PAPER

THE EFFECT OF SUSPENSION-LINE LENGTH
ON VIKING PARACHUTE INFLATION LOADS

Prepared by

Theodore A. Talay
Theodore A. Talay

Lamont R. Poole
Lamont R. Poole,

and

Charles H. Whitlock
Charles H. Whitlock

Approved by Clarence S. Ellis
for Don D. Davis, Jr., Chief
Space Technology Division

Approved for
distribution by Robert H. Wright
for Clifford H. Nelson
Director for Space

LANGLEY RESEARCH CENTER

NATIONAL AERONAUTICS AND SPACE ADMINISTRATION

THE EFFECT OF SUSPENSION-LINE LENGTH
ON VIKING PARACHUTE INFLATION LOADS

By Theodore A. Talay, Lamont R. Poole,
and Charles H. Whitlock

SUMMARY

Analytical calculations have considered the effect on maximum load of increasing the suspension-line length on the Viking parachute. Results indicate that unfurling time is increased to 1.83 seconds from 1.45 seconds, and that maximum loads are increased approximately 5 percent with an uncertainty of -4 percent to +3 percent.

INTRODUCTION

Wind-tunnel tests have shown that the effect of the blunt Viking entry vehicle is to reduce the drag forces produced by the parachute decelerator. As a result, the suspension lines on the Viking parachute were recently lengthened to move the canopy farther rearward in the wake of the entry vehicle. The result is increased drag produced by the parachute to meet mission design requirements. The effect of the increase in suspension-line length on the opening load is unknown. It is the purpose of this document to define the effects of suspension line length on this design parameter.

Specifically, the effects of suspension-line length change will be examined in the Min $H_{p,s}$ atmosphere which is the worst-case load condition on which the parachute is designed. First, trajectory effects will be defined in that the differences in the length of time for parachute unfurling will be examined. Trajectory conditions at the end of unfurling will provide the initial conditions for the inflation process. Next, the effect of suspension-

line length on the opening loads felt both at the entry vehicle and on the canopy will be analyzed. The relative effects of uncertainties in opening load magnitude, suspension system damping, and wind-tunnel test results will be considered.

BES units are used throughout this document to simplify application of the results to the Viking Project.

SYSTEM DESCRIPTION

The total deployment process for the Viking decelerator consists of an unfurling phase and an inflation phase as shown in figure 1. Unfurling is the phase in which the parachute is strung out from the deployment bag in a lines-first manner following mortar fire. The canopy inflation phase is assumed to begin at the end of the unfurling process. Overall dimensions for the Viking decelerator system were taken from reference 1 and are shown in figure 2. The distribution of weight along the parachute strung-out length is shown in figure 3. Suspension line and bridle material force-elongation characteristics are presented in figure 4. These static data were obtained using unsterilized material in tests at the Langley Research Center. Manual pull tests were used to define characteristics for loads under 50 pounds. These results were then combined with Instron test data for loads above 50 pounds. Damping characteristics of suspension-system material are presently undefined. For purposes of this analysis, an average value of damping will be assumed. Final results will then be compared for several values of damping to examine sensitivity. A constant damping coefficient value of 25 pound-seconds is assumed for each suspension line. This coefficient is the ratio of the force caused by damping to the strain rate (in percent per second). The bridle

material is assumed to have zero damping, and each leg is considered to have four layers of material for computation of force-elongation characteristics for the total bridle assembly.

Entry vehicle and decelerator mass and aerodynamic properties assumed for this analysis are given in the table.

SIMULATION AND RESULTS

Program Inputs

The unfurling sequence is simulated using the analytical model described in reference 2. Entry vehicle and decelerator physical properties are used as program inputs. Initial conditions to begin the unfurling computations were taken from reference 3 for the Min $H_{p,s}$ atmosphere and were adjusted for different atmospheric properties from reference 4. The adjusted initial conditions for mortar fire are Mach number equal 2.2, dynamic pressure equal 10.55 pounds per square foot, and flight path angle equal -10.81 degrees. For the $X/D = 6.03$ configuration, a mortar velocity of 90 feet per second is used for consistency with reference 3. A mortar velocity of 98 feet per second is used for the $X/D = 8.69$ configuration based on current mortar system design. An increased ejection velocity is required to insure completion of the unfurling process when the length of the system is increased.

The inflation sequence is simulated using a currently unpublished analytical model. The model considers nonlinear elastic properties with suspension-system geometry corrections as a function of instantaneous canopy diameter. As usual in most models of elastic systems, the weight of the canopy is considered attached to a massless spring, the suspension-system. The model also considers the effect of entry vehicle-decelerator relative

velocity in the computation of dynamic pressure acting on the parachute canopy. Geometry changes during inflation are prescribed by the canopy projected-diameter profile shown in figure 5. This curve was constructed using data from the Planetary Entry Parachute Project. The $C_D S$ history shown in figure 6 is estimated for the $X/D = 6.03$ configuration. A $C_D S$ history relative to the figure 6 history will be defined for the $X/D = 8.69$ configuration during this study. Final results will be compared for several different magnitudes of the figure 6 $C_D S$ history to examine the effects of uncertainty in opening load magnitude.

Program Results

Unfurling Sequence.- The effect of longer suspension lines is to increase the unfurling time between the events of mortar fire and bag strip. For the Viking system, however, the difference is not great because the mortar velocity is increased from 90 to 98 feet per second. Figure 7 shows the unfurled length as a function of time for both the $X/D = 6.03$ and 8.69 configurations. These curves show that unfurling time is increased to 1.83 seconds from 1.45 seconds by lengthening the suspension lines. The effect of longer unfurling time is to reduce the Mach number and dynamic pressure at bag strip by 0.02 and 0.12 pounds per square foot, respectively. Thus, the inflation process begins at slightly less severe conditions for the $X/D = 8.69$ configuration.

Inflation Sequence.- Initial inflation calculations were completed using the figure 6 $C_D S$ history for both the 6.03- and 8.69-length configurations. Inflation load histories for both the canopy and entry vehicle are presented in figure 8. From these curves, it should be noted that the maximum loads experienced by the canopy are 5.8 percent higher than those of the vehicle

for the $X/D = 6.03$ configuration and 6.3 percent higher for the $X/D = 8.69$ system given the same $C_D S$ curve. Thus, increased suspension line length attenuates the loads transmitted to the entry vehicle by only a small amount.

It should be observed in figure 8 that the maximum vehicle load for the $X/D = 8.69$ system is approximately 4 percent lower than the load on the $X/D = 6.03$ system. Approximately 1 percent of this amount is because inflation begins at a slightly lower dynamic pressure for the long configuration. The remaining reduction is caused by the fact that longer suspension line lengths cause increased stretch velocities during inflation. The increase in relative velocity between the vehicle and decelerator causes reduced dynamic pressures and loads at the canopy. This in turn means lower loads at the vehicle for increased suspension line length if the $C_D S$ history of the canopy is unchanged.

For the Viking system, the $C_D S$ history of the canopy is not identical for both parachute configurations. The $X/D = 8.69$ system has the parachute farther rearward in the wake to produce more drag. For this reason, it is expected that the $C_D S$ values for that configuration should be larger than the figure 6 curve. An appropriate $C_D S$ history for the 8.69 configuration can be derived using preliminary wind-tunnel data from recently completed tests at AEDC. The indirect procedure used to derive canopy drag area from vehicle-location measurements is described in the following paragraph.

Parachute inflation loads were measured for X/D values 6.0 and 8.5 at Mach number 2.2 in the AEDC-PWT facility. Preliminary results indicate that the nondimensional opening load parameter measured at the vehicle is 6.2 percent higher for the 8.5 configuration than the 6.0 system. Thus if all other factors were equal, the canopy $C_D S$ curve should be adjusted until the vehicle forces are larger for the long system than the short system by 6.2 percent.

Unfortunately all other factors are not equal because of trajectory differences. Unfurling calculations indicate that the longer system begins inflation at a dynamic pressure 1.2 percent lower than the short system. Thus to equal the 6.2 percent load difference measured in the wind tunnel, the $X/D = 8.69$ canopy drag area curve should be adjusted until the vehicle loads for the long system are 4.8 percent larger than those of the $X/D = 6.0$ configuration. Using an iteration procedure, an approximate adjustment was made and the C_{DS} history shown on figure 9 was derived for the $X/D = 8.69$ configuration. The important point to note is that a 10.0 percent increase in canopy C_{DS} is required to achieve 4.7 percent higher vehicle loads for the long system over the short system.

An increase of 10 percent in C_{DS} does not mean canopy loads are increased by an equal amount when suspension lines are lengthened. As C_{DS} is increased, differences in the trajectory profiles and the dynamic pressure reduction caused by stretch velocity are amplified. The actual loads felt in the system are given below:

Configuration	Vehicle Load (lbs)	Canopy Load (lbs)
$X/D = 8.69$	13 296	14 077
$X/D = 6.03$	12 706	13 419
Ratio	1.047	1.049

These results indicate that when both trajectory and elastic differences are taken into account, actual loads increase only approximately 5 percent both at the canopy and vehicle when suspension lines are lengthened.

EFFECTS OF UNCERTAINTIES

The previous results are based on an assumed average value of damping and an estimated canopy $C_D S$ history for the $X/D = 6.03$ configuration (figure 6). The effects of uncertainties in these parameters are shown in figures 10, 11, and 12. Figure 10 shows the ratios of loads between the two configuration for values of the average damping coefficient between 0 and 50 pound-seconds. The uncertainty in damping coefficient causes an uncertainty of -3 percent to +1 percent about the nominal 5 percent value. Figure 11 shows the effect of damping on the ratio of loads between the canopy and the vehicle. These curves indicate that damping has a significant effect on the distribution of loads between the canopy and vehicle. It also significantly influences the magnitude of loads experienced by the canopy.

The effect of uncertainty in the baseline $C_D S$ history assumed for the $X/D = 6.03$ configuration is shown in figure 12. Values are shown as a function of maximum vehicle loading to increase the usefulness of results. The figure 6 $C_D S$ curve was adjusted by use of a multiplier to higher values to simulate unknown Mach number or wake effects. As baseline $C_D S$ is adjusted up the loads on the $X/D = 6.03$ vehicle are also increased. Thus the abscissa of figure 12 represents the effect of uncertainty in the baseline $C_D S$ history. The $C_D S$ history for the $X/D = 8.69$ system was adjusted such that it was always 10 percent above the $X/D = 6.03$ history to remain consistent with wind-tunnel results. The curves in figure 12 indicate that the uncertainty in baseline $C_D S$ causes an uncertainty of -2 to +0 percent in the nominal 5 percent value. Figure 13 shows the actual vehicle loads for the long configuration as a function of those expected in the short system when the damping coefficient is equal 25 pound-seconds.

The analysis of this document is highly dependent on opening load data obtained from the Mach 2.2 parachute tests at AEDC. The relative C_D histories between the two parachute configurations are based on the fact that the opening load parameter measured at the vehicle for the long parachute was 6.2 percent higher than that for the short configuration. Examination of the analog plots from the tunnel tests indicate that the uncertainty about the 6.2 percent value is -1 percent to +3 percent. This uncertainty will feed almost directly into the results of this document.

An uncertainty level considering the combined effect of all parameters may be estimated using the root-sum-square technique. Based on the above uncertainty levels for suspension material damping, baseline C_D history, and wind-tunnel results, the combined uncertainty level for the 5 percent load increase as a result of lengthening the Viking parachute's suspension lines is -4 percent to +3 percent.

CONCLUSIONS

Analytical calculations have considered the effect on maximum load of increasing the suspension-line length on the Viking parachute. Complex interactions between the trajectory environment and decelerator elastic characteristics have been simulated for the Min $H_{p,s}$ atmosphere. Based on the results of this study, the following conclusions are made:

1. Decelerator unfurling time is increased to 1.83 seconds from 1.45 seconds and the Mach number and dynamic pressure at bag strip are reduced 0.02 and 0.12 pounds per square foot, respectively.

2. Maximum loads at both the canopy and vehicle are increased approximately 5 percent with an uncertainty of -4 percent to +3 percent.

It should be noted that design changes in the Viking system can invalidate the results of this study. The calculations are particularly sensitive to significant changes in deployment conditions, mortar ejection velocities, entry vehicle ballistic coefficient, and decelerator physical properties.

REFERENCES

1. Goodyear Aerospace Corp. Drawings No. 3064130-102 and 3064110-104.
2. Poole, Lamont R.; and Huckins, Earle K. III: An Approximate Technique for Analyzing the Effects of Suspension-Line Elasticity During the Parachute Unfurling Process. Prospective NASA TN.
3. Moog, R.D.: Viking Dynamics Data Book, VER-19. Martin Marietta Corp. TR-3720052, Revision A, April 1971.
4. Mars Engineering Model. Viking 75 Project Document M75-125-1, December 1970.

TABLE

Mass and Aerodynamic Properties

Weight-Earth pounds

Entry vehicle	1888	
Parachute	X/D = 6.03	X/D = 8.69
Canopy	46.15	46.15
Suspension lines	23.31	30.73
Bridle	6.00	6.00
Total	<u>75.46</u>	<u>82.88</u>

Entry Vehicle Drag Coefficient

Mach	C_D
0	1.081
.3	1.081
.6	1.111
1.0	1.322
1.4	1.552
2.0	1.597
3.0	1.612
4.0	1.617
6.0	1.622

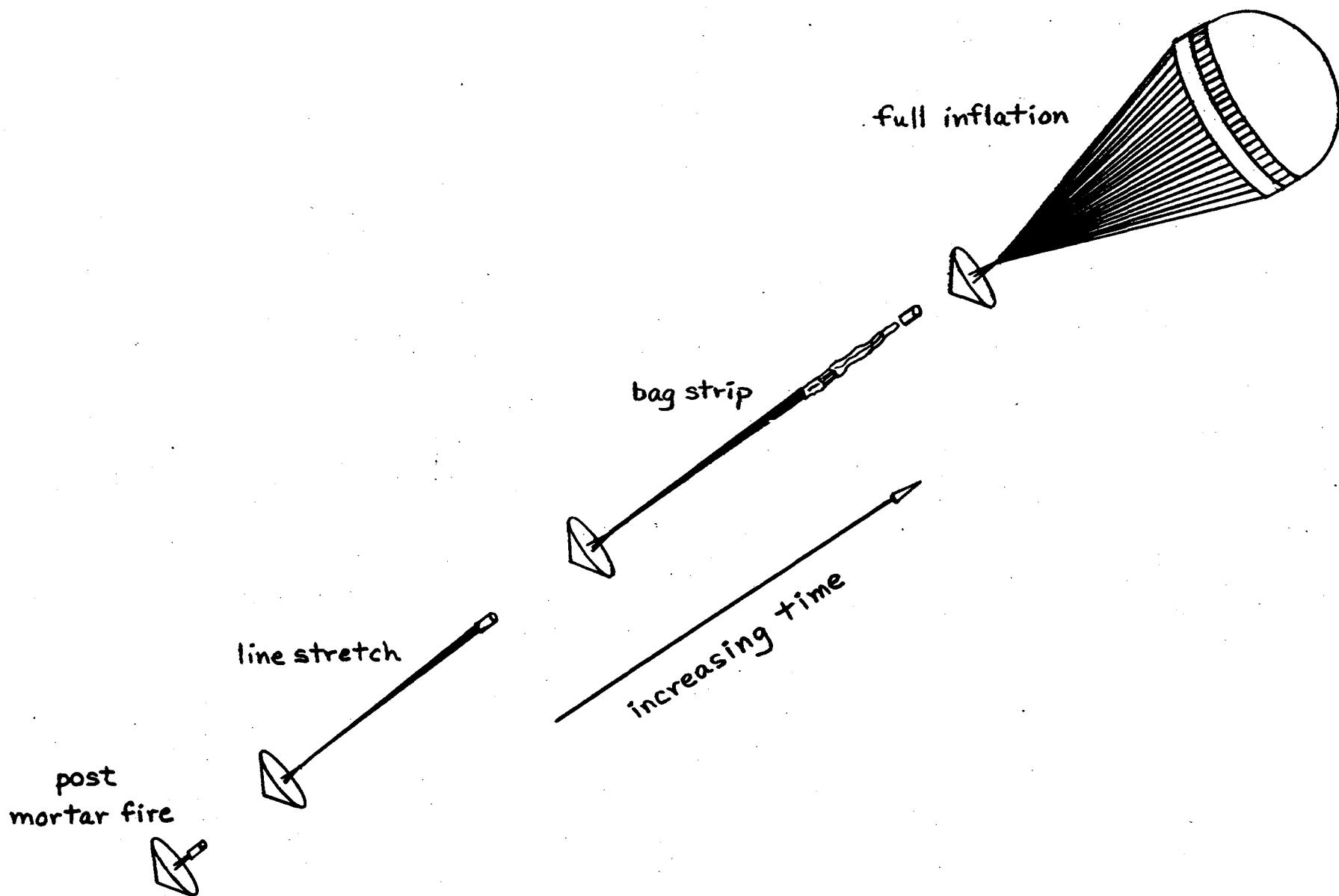
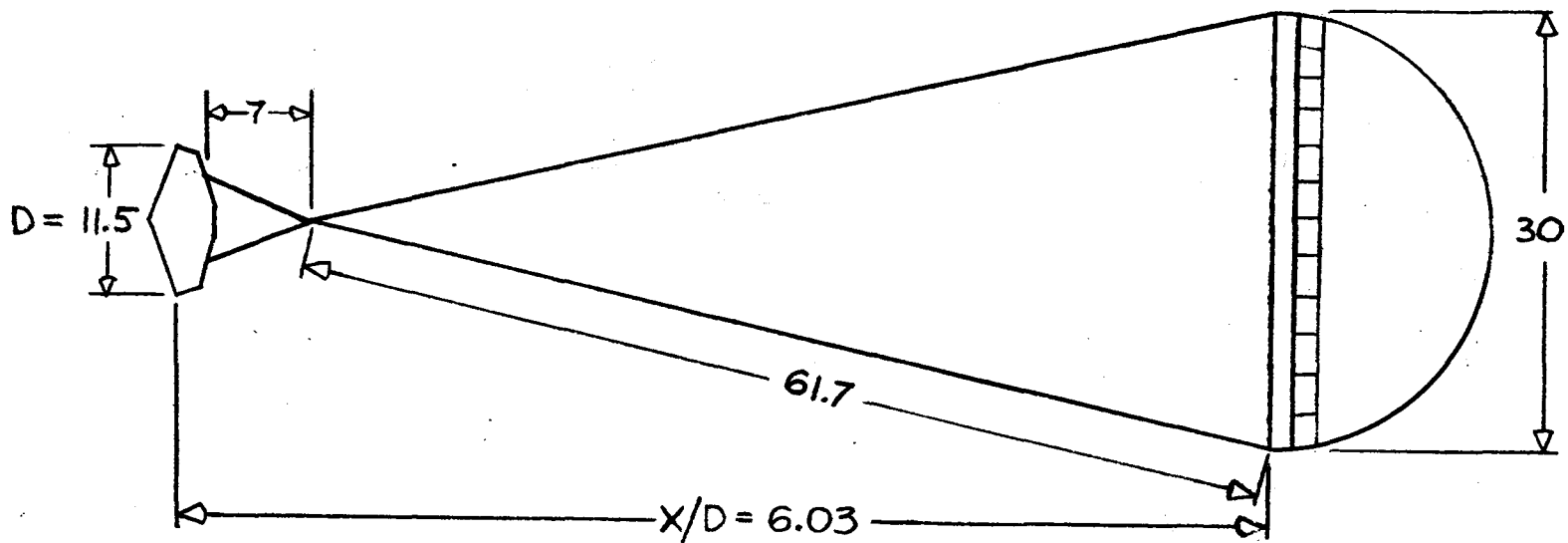
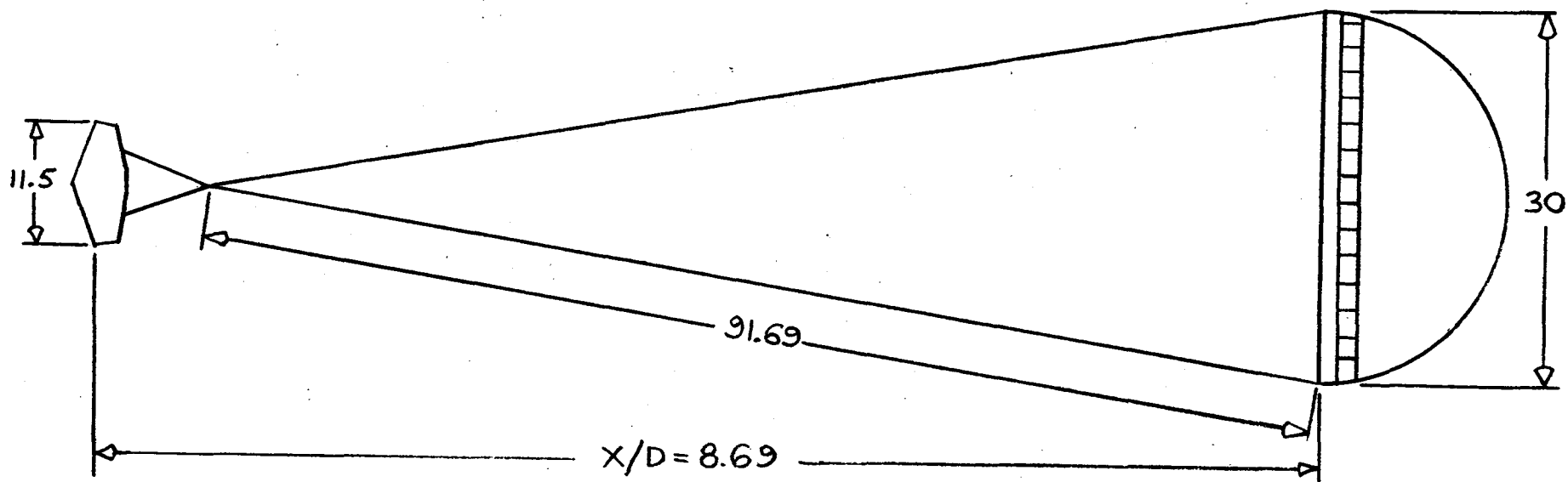


Figure 1.- Sketch of unfurling and inflation sequence.



(a) Previous configuration



(b) Current configuration

Figure 2.- System description for Viking configurations.

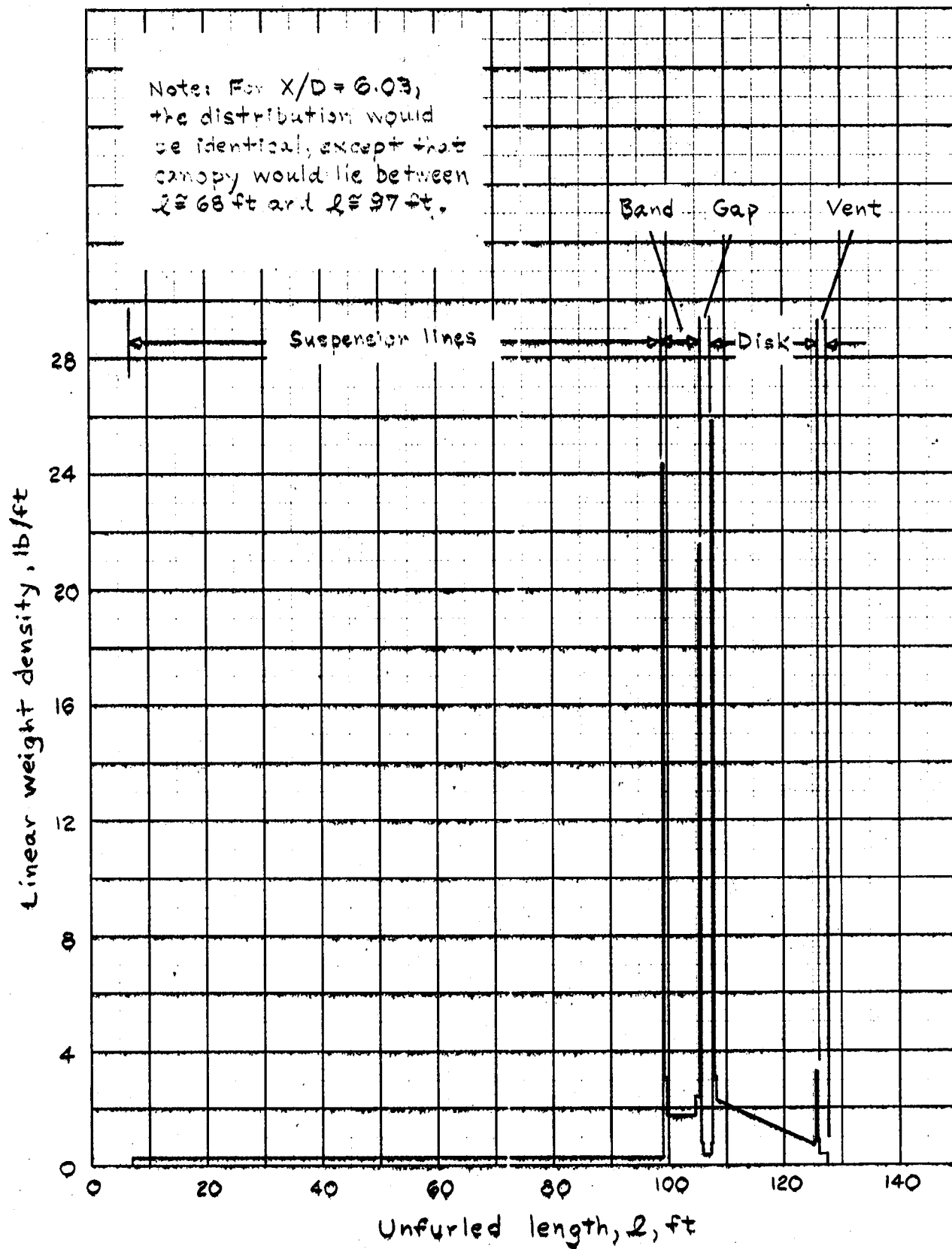
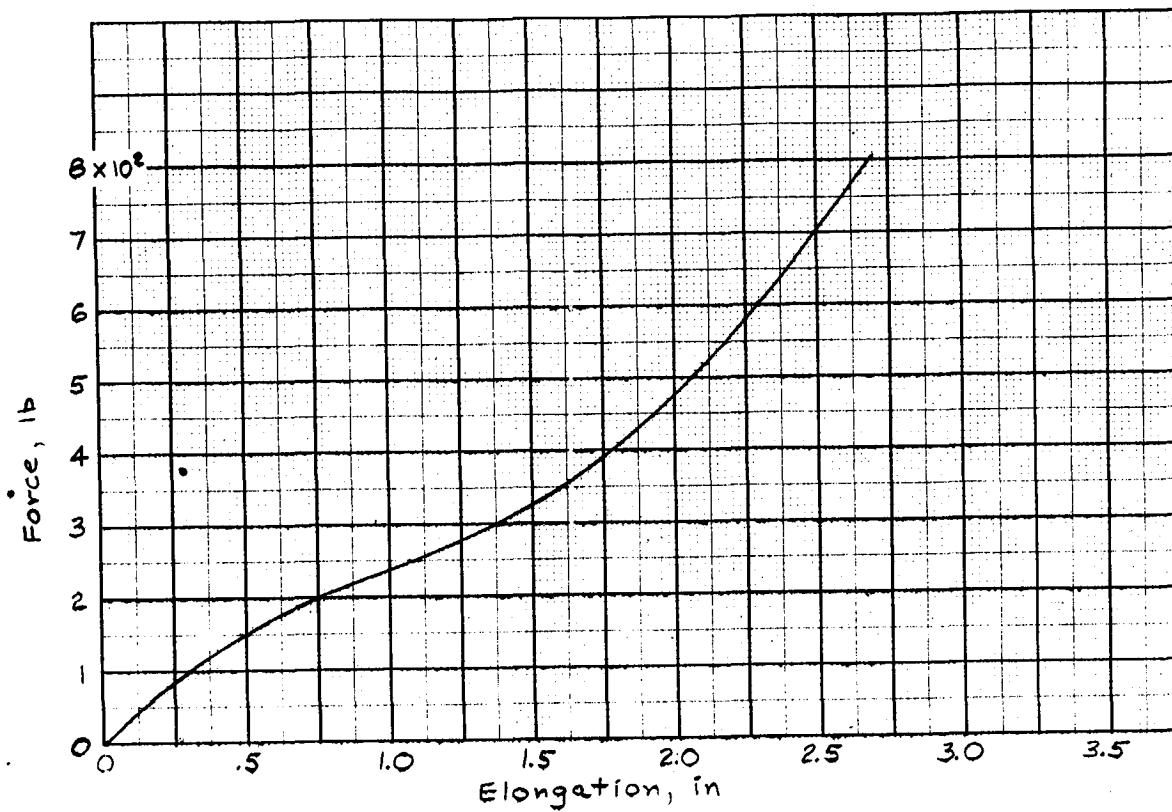
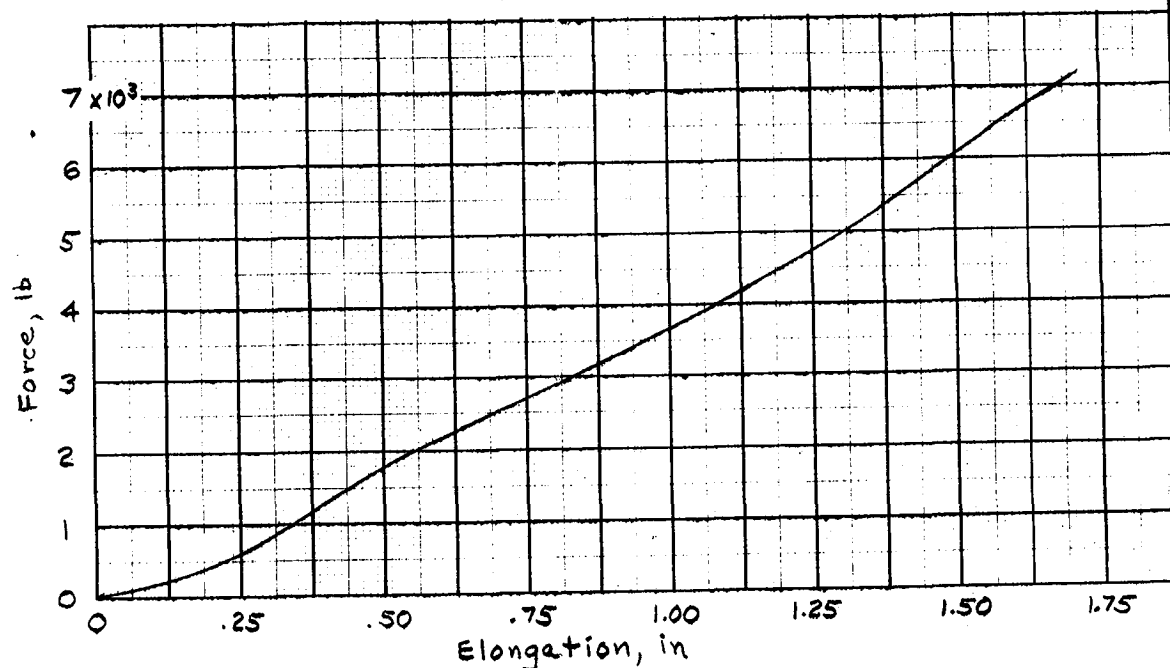


Figure 3.- Linear weight distribution of Viking 53-ft.- D6 DGB, X/D at full inflation = 8.69.



(a)- Viking suspension line sample



(b)- Viking bridle material sample

Figure 4.- Force-elongation curves for Viking suspension line and bridle samples, as obtained from Instron tests (gage length ≈ 10 in).

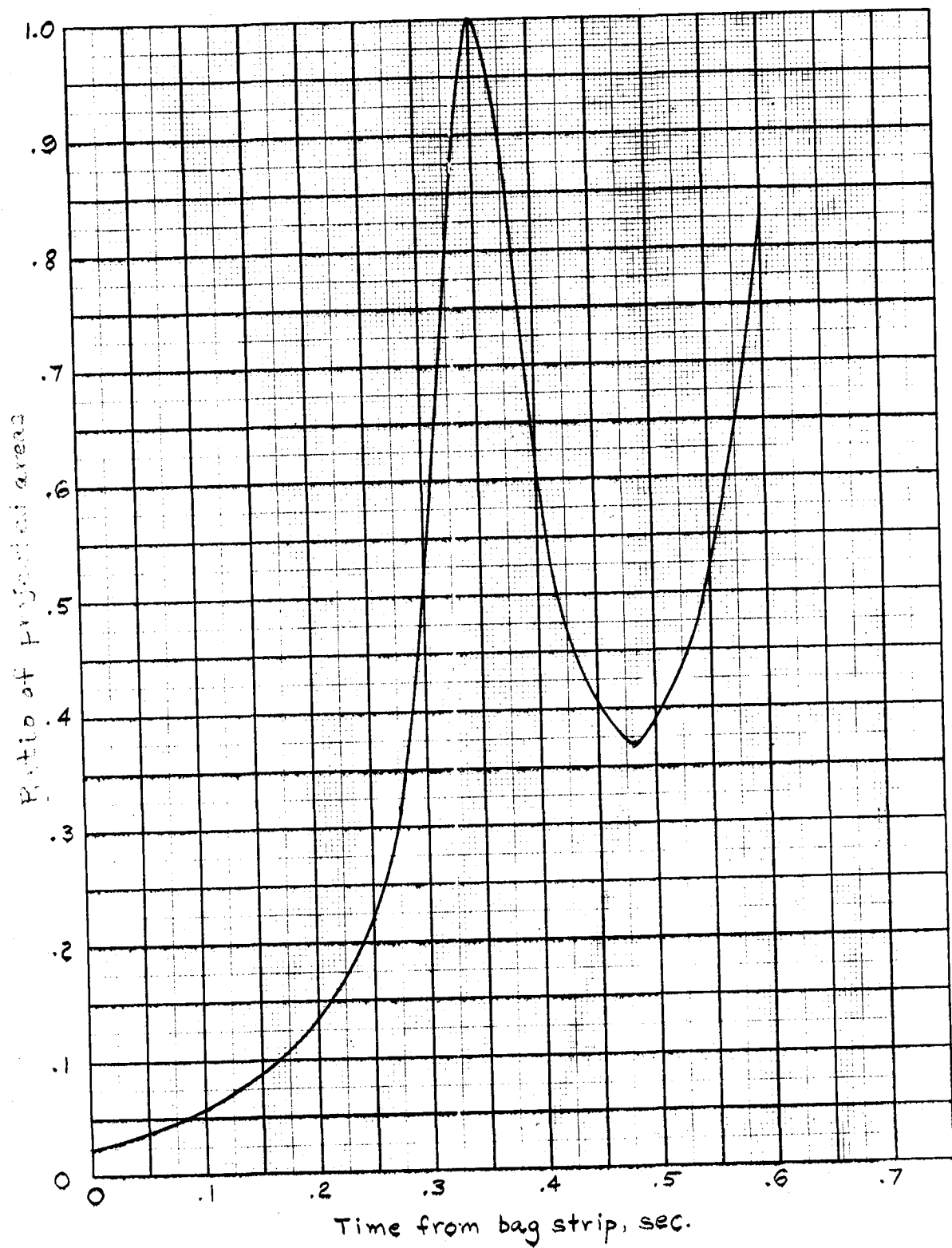


Figure 5.- Input ratio of instantaneous canopy projected area to canopy projected area at full inflation.

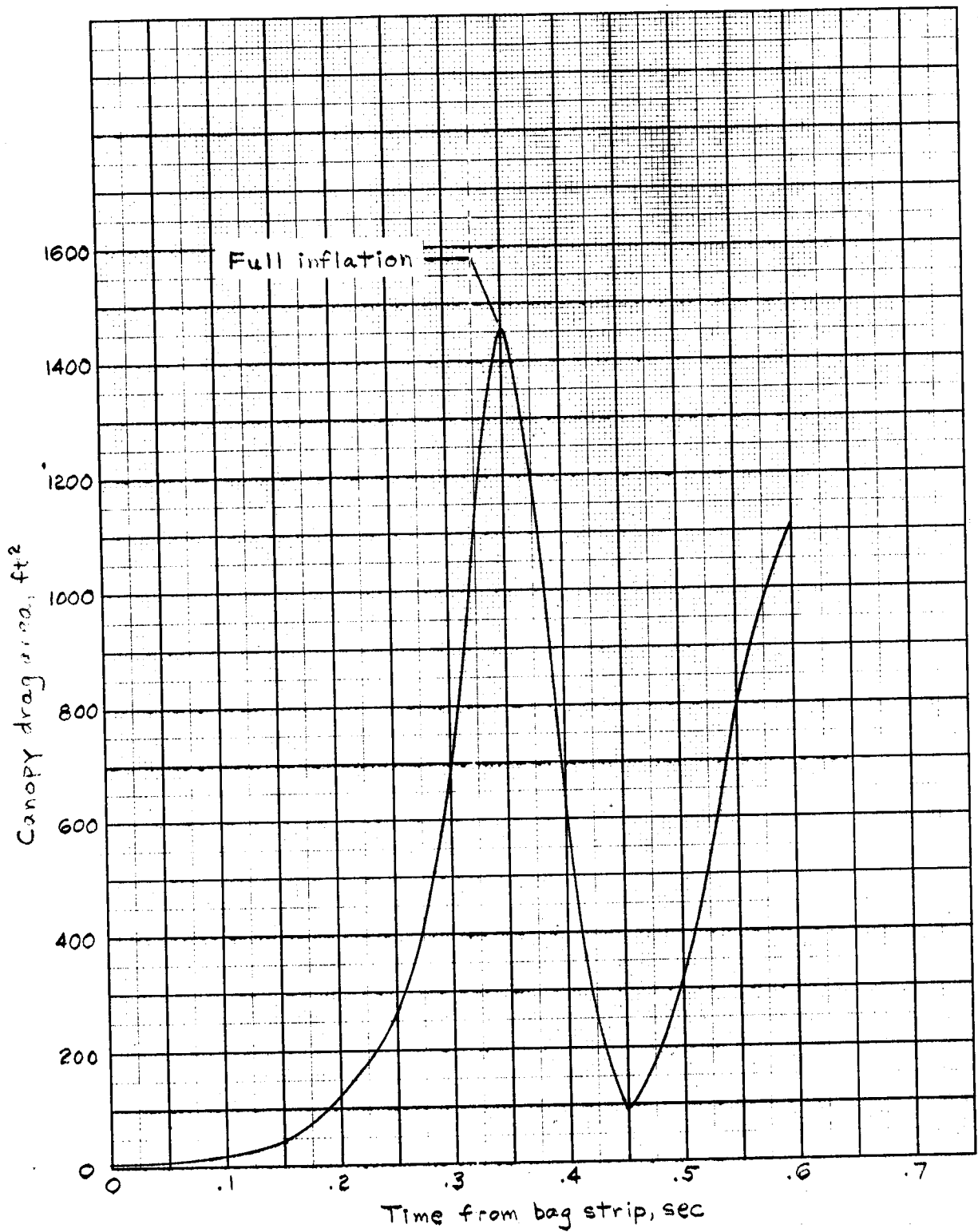
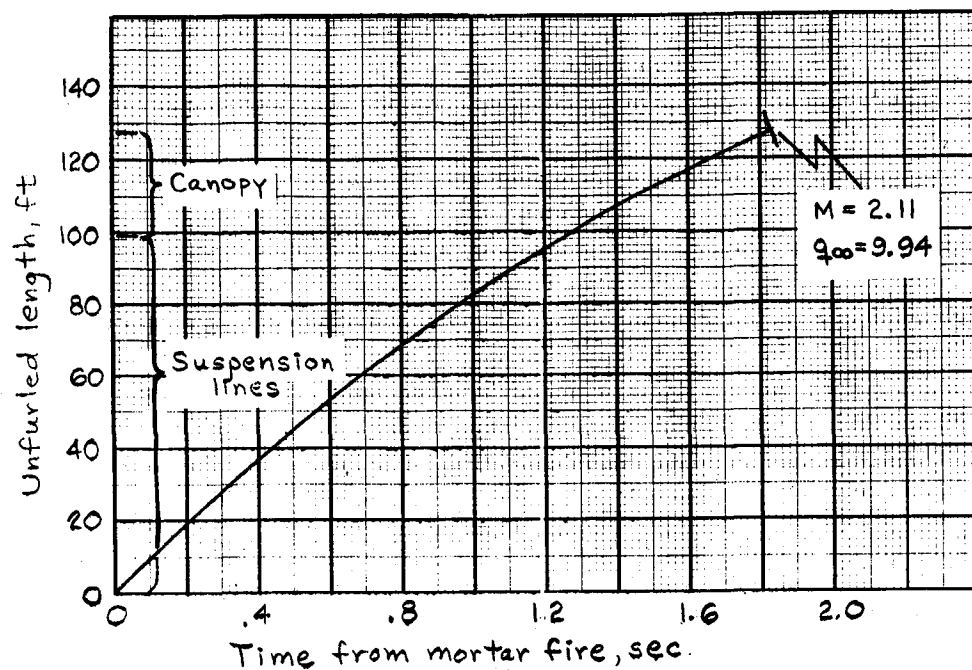
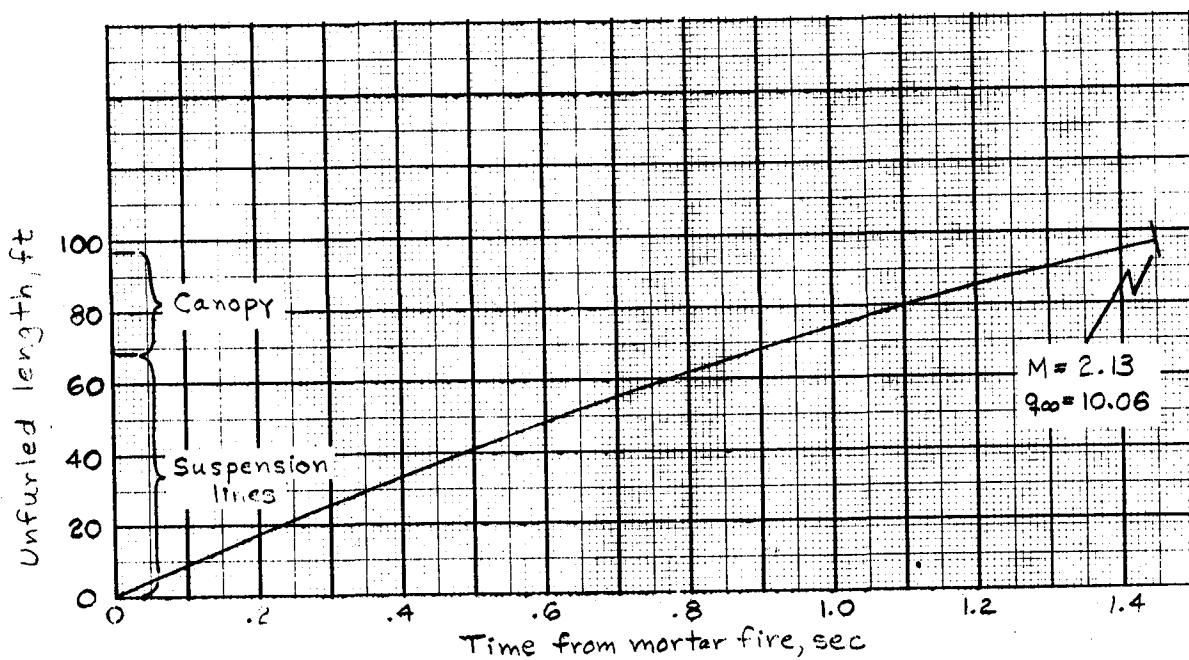


Figure 6.- Input canopy drag area history during inflation of the Viking 53-ft- D_0 DGB, $X/D = 6.03$.

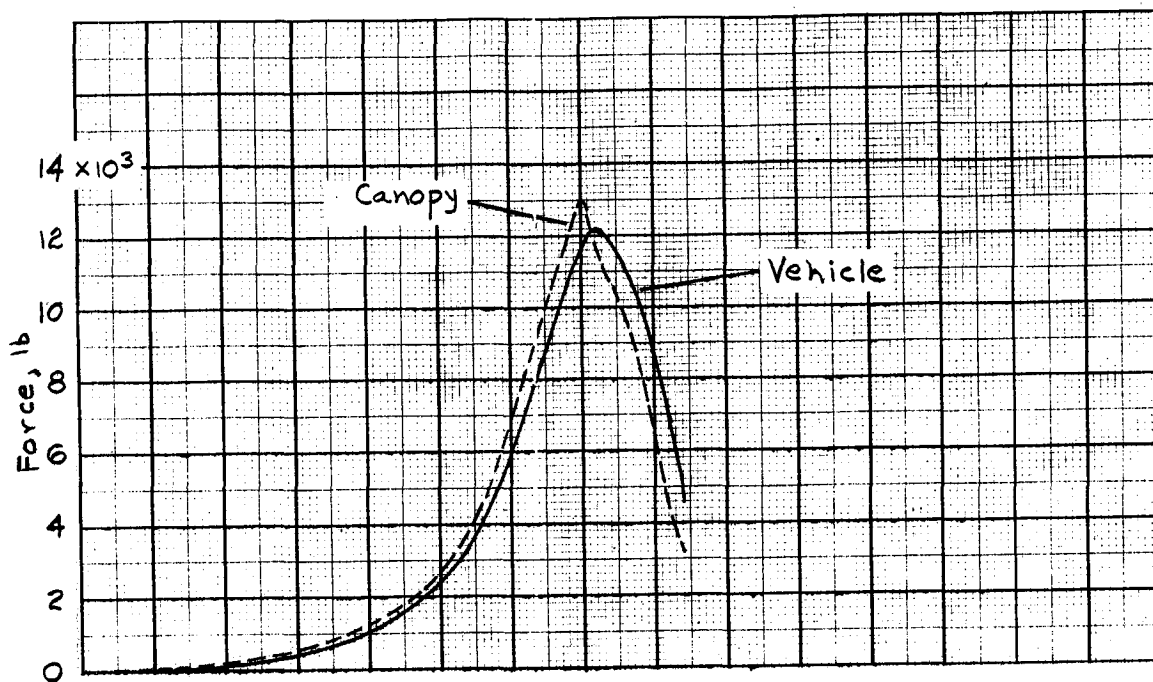


(A) $X/D = 8.69$, mortar velocity = 98 fps

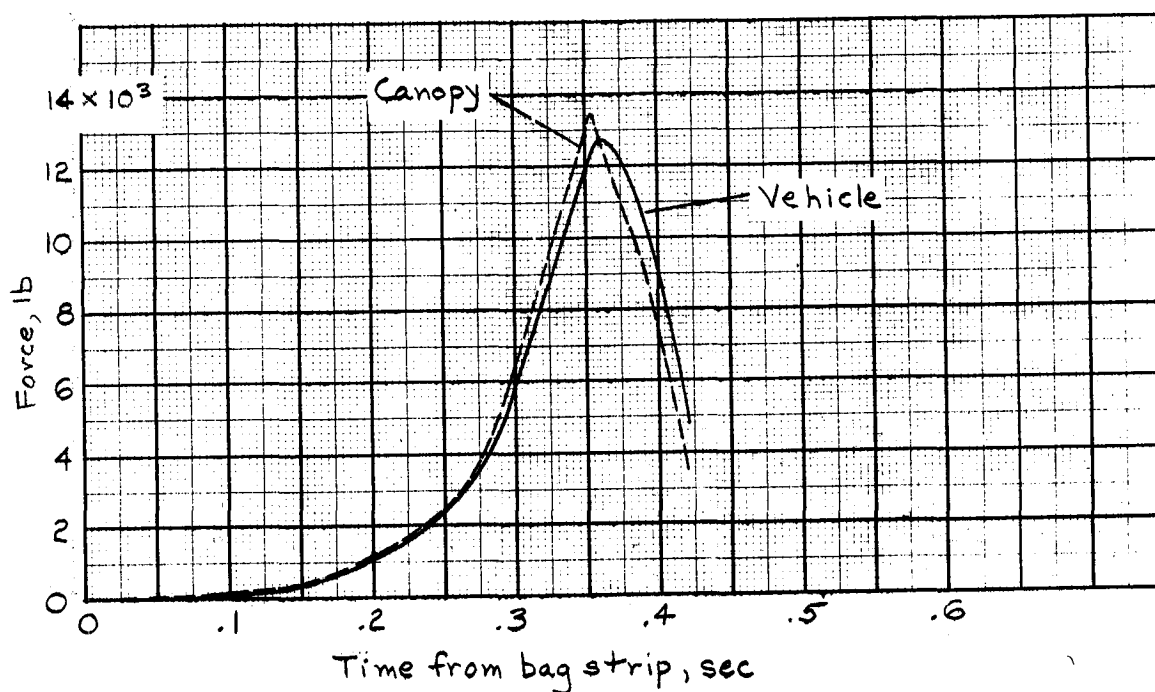


(B) $X/D = 6.03$, mortar velocity = 90 fps

Figure 7.- Unfurling histories for Viking configurations in Min Hp,s atmosphere; $M_{\text{mortar fire}} = 2.2$, $q_{\infty \text{ mortar fire}} = 10.55$.



(a) $X/D = 8.69$



(b) $X/D = 6.03$

Figure 8.- Inflation loads for two configurations using typical C_D history (Figure 6); damping coefficient = 25 lb-sec/line.

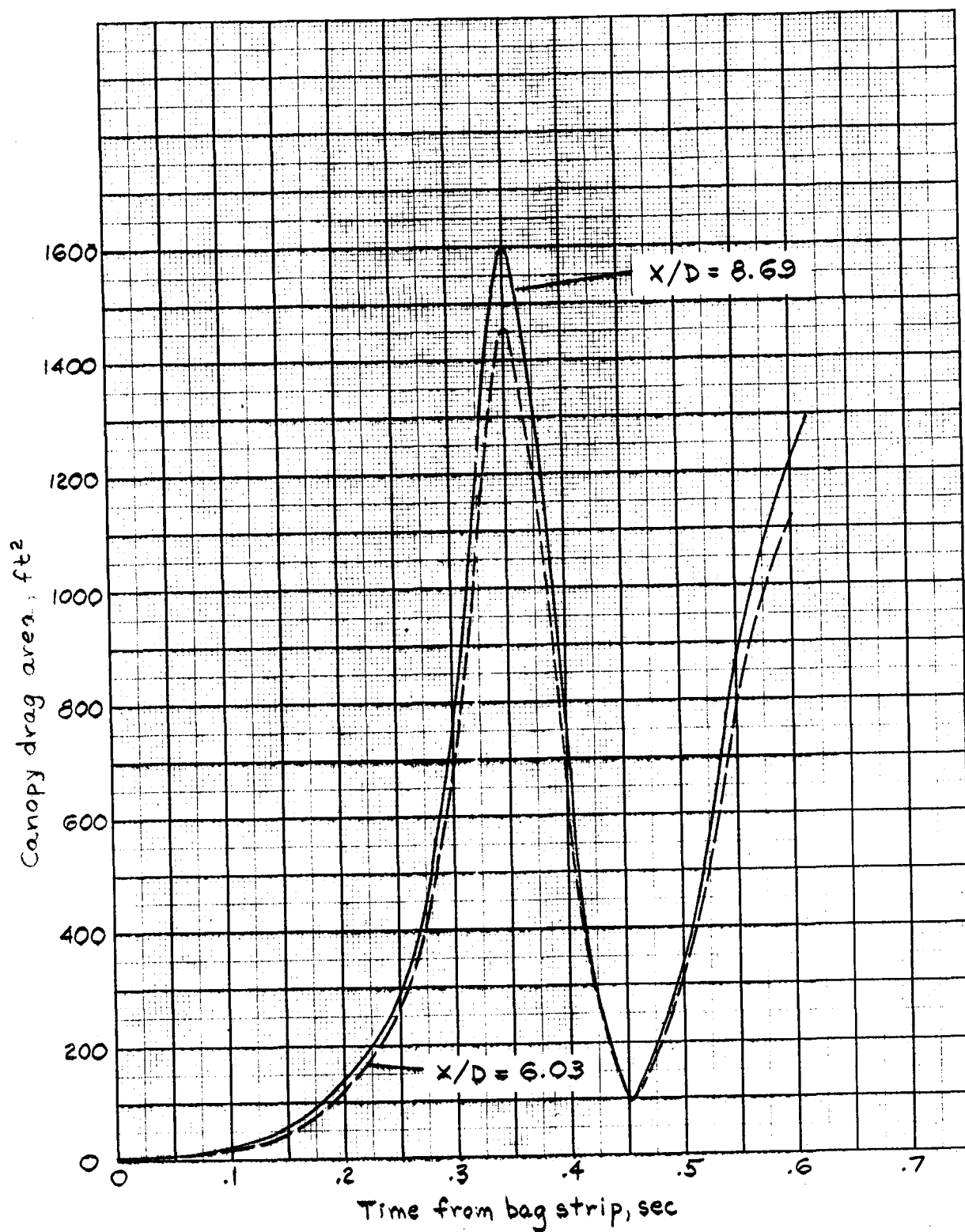


Figure 9.- Revised $C_D S$ history for $X/D = 8.69$ configuration.

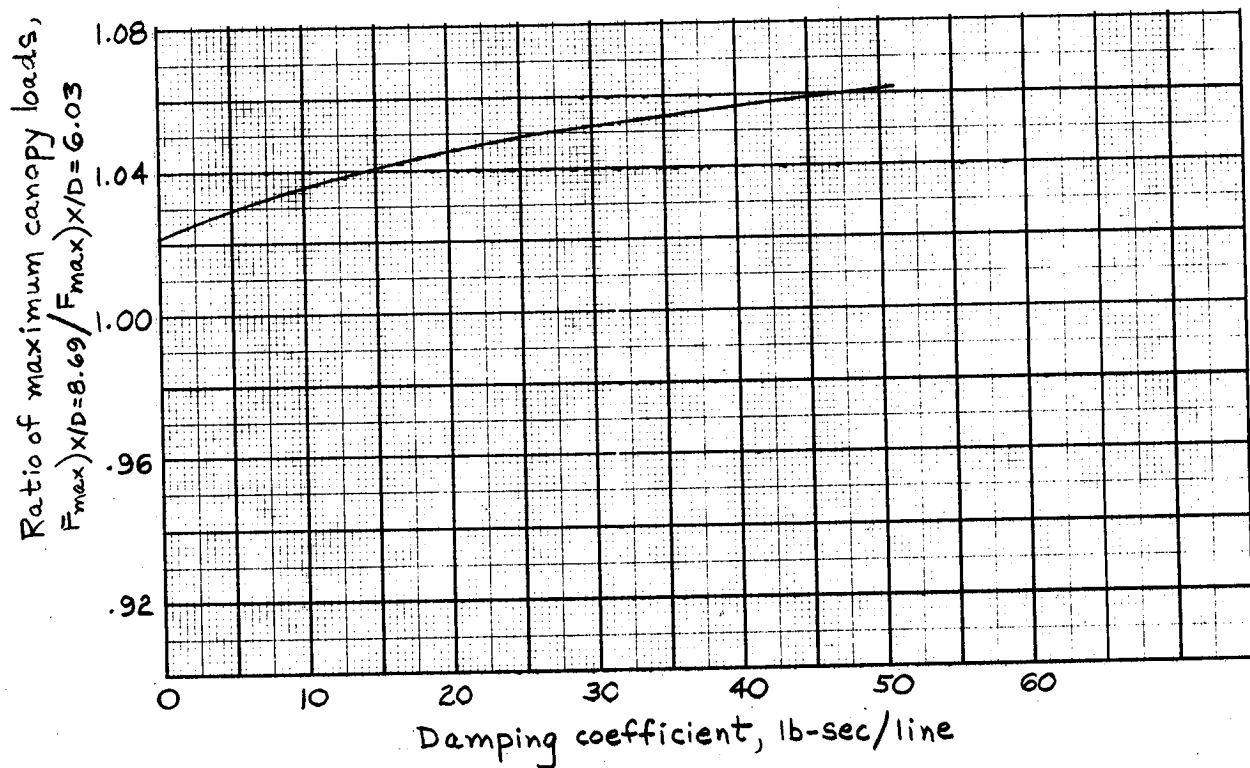
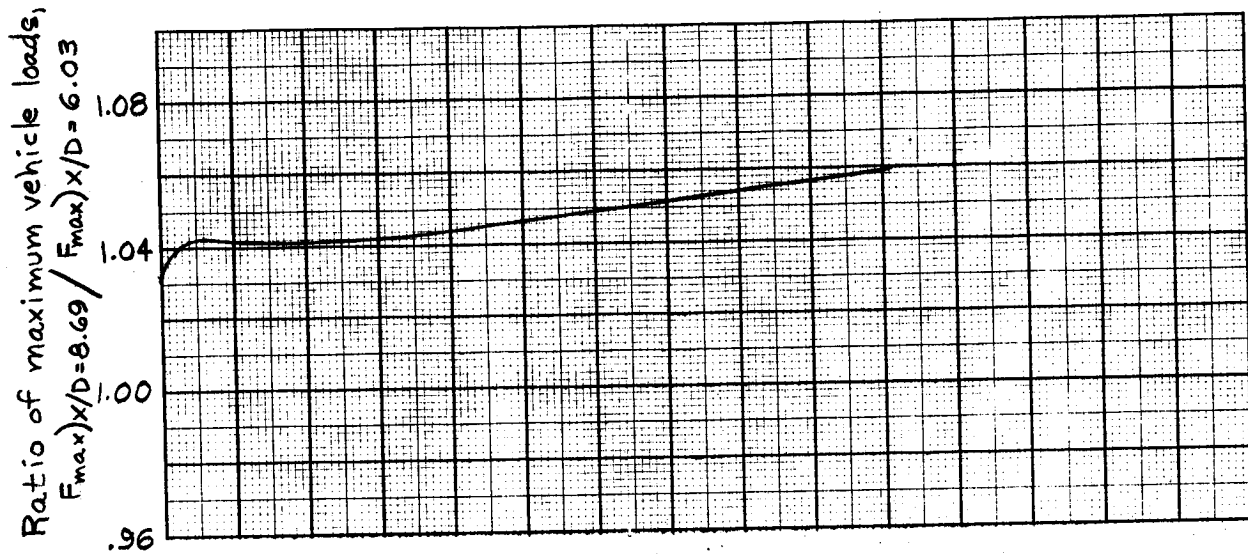
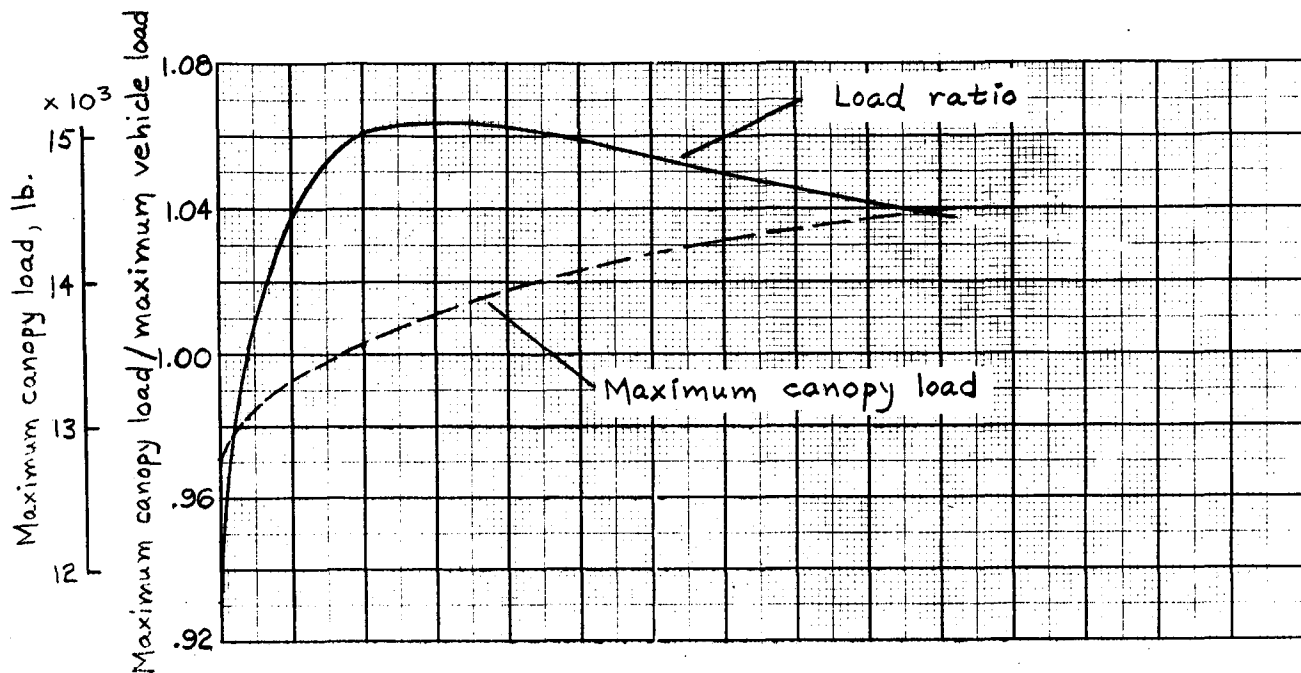
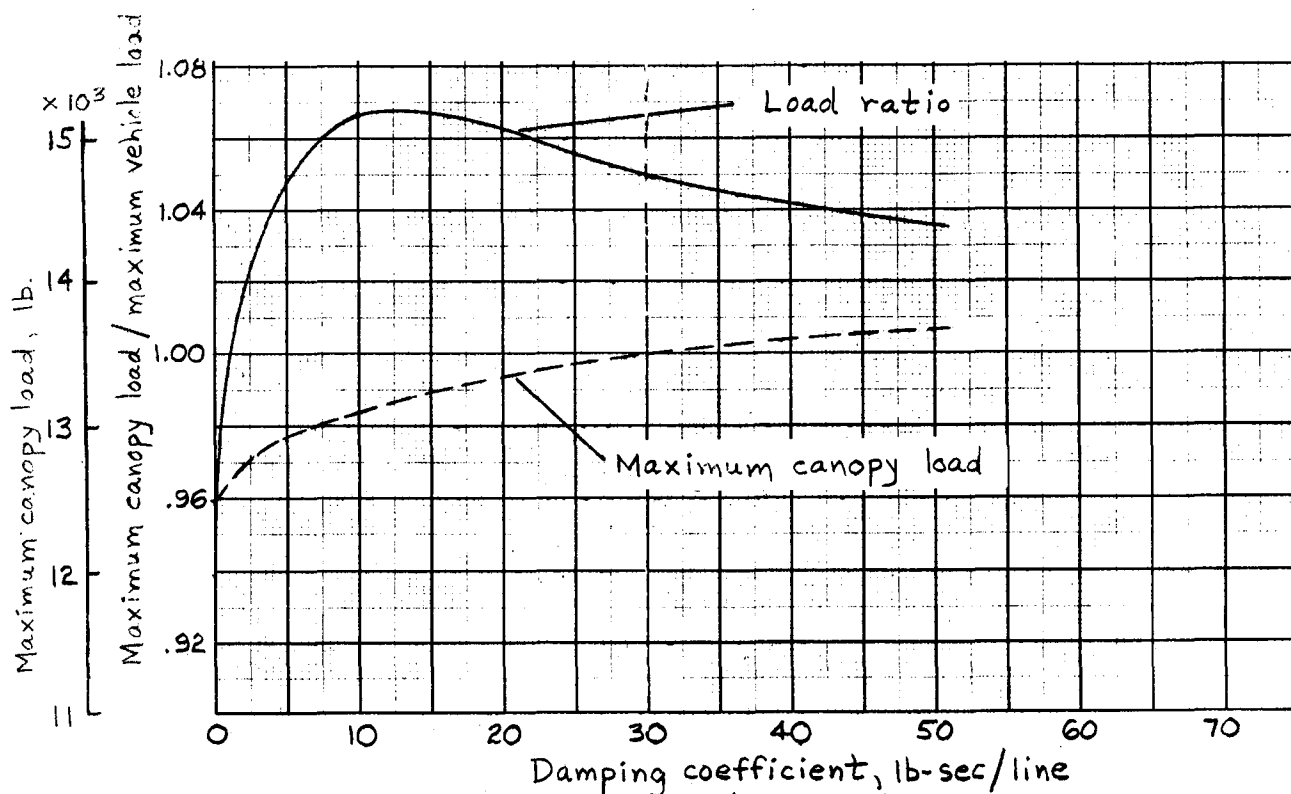


Figure 10.— Ratios of maximum loads for the two Viking configurations as a function of suspension line damping coefficient.



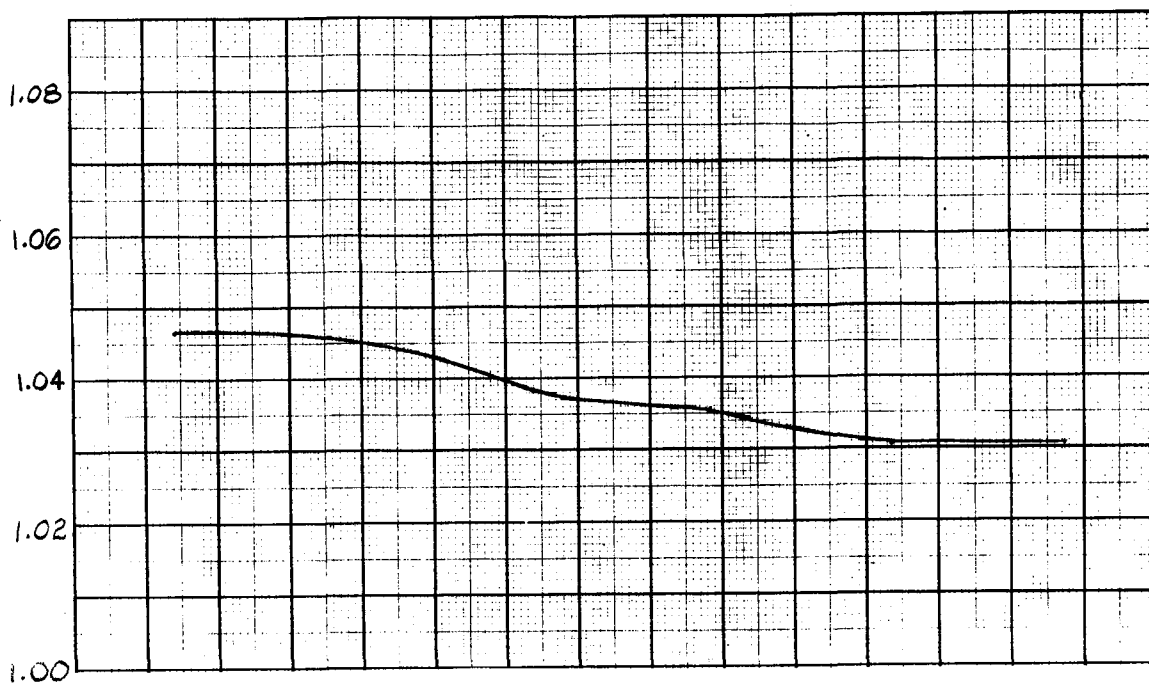
(a) $X/D = 3.69$



(b) $X/D = 6.03$

Figure 11.— Ratio of maximum canopy load to maximum vehicle load, for two Viking configurations, as a function of suspension line damping coefficient.

Ratio of max. vehicle loads for $X/D=8.69$
to max. vehicle loads at $X/D=6.03$.



Ratio of max. canopy loads for $X/D=8.69$
to max. canopy loads for $X/D=6.03$.

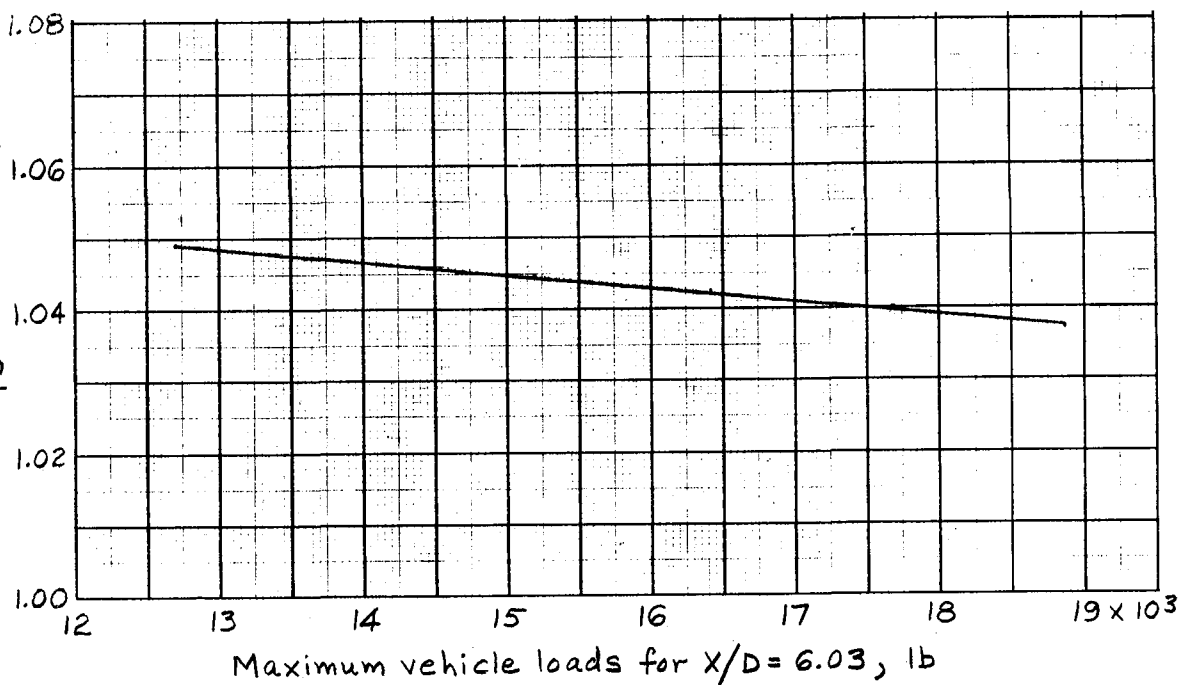


Figure 12.- Ratios of maximum canopy loads and maximum vehicle loads for two Viking configurations, as a function of maximum vehicle loads for the $X/D=6.03$ configuration.

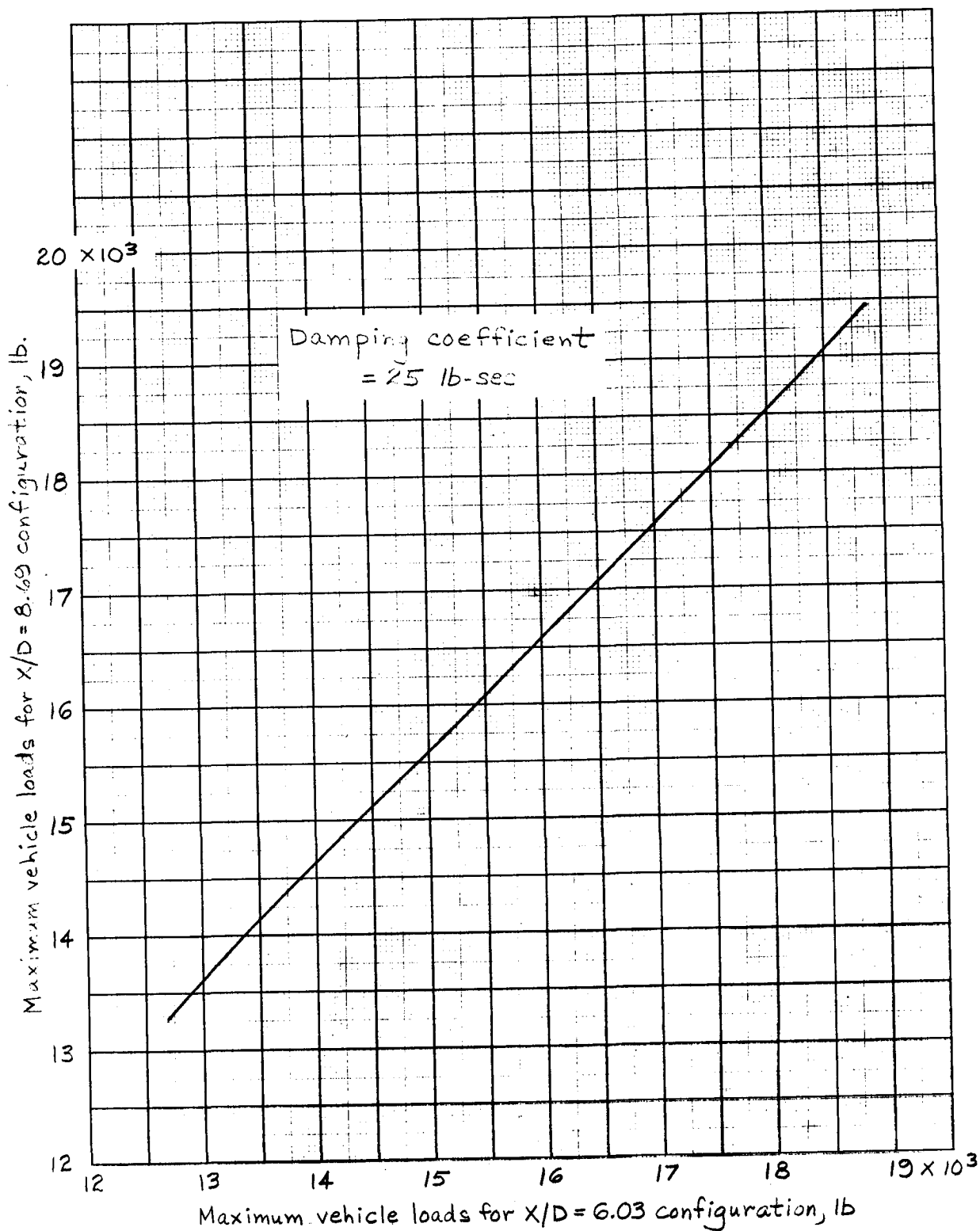


Figure 13.- Maximum vehicle loads for $X/D = 8.69$ configuration versus maximum vehicle loads for $X/D = 6.03$ configuration.